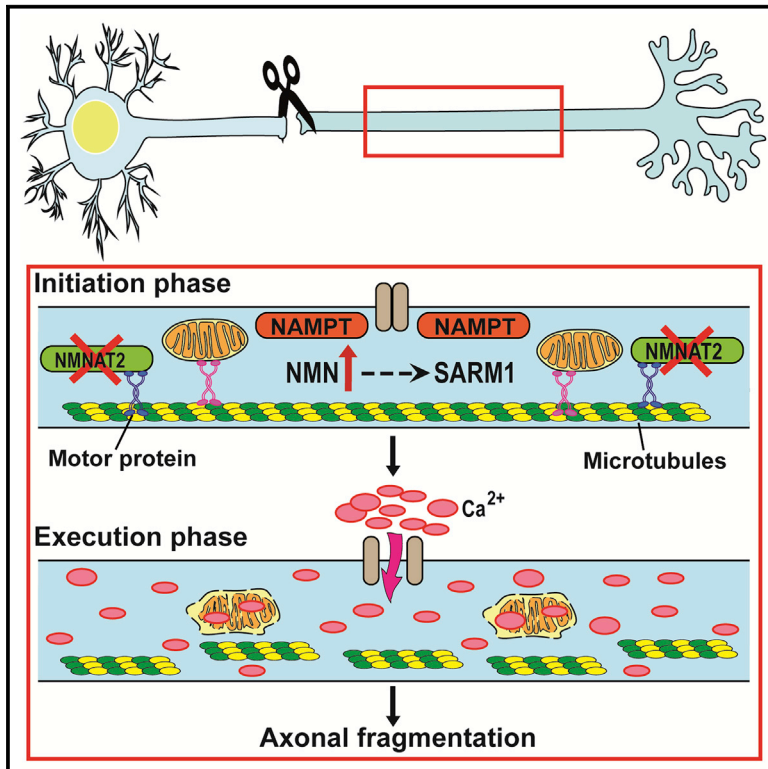


Wallerian Degeneration Is Executed by an NMN-SARM1-Dependent Late Ca^{2+} Influx but Only Modestly Influenced by Mitochondria

Graphical Abstract



Authors

Andrea Loreto, Michele Di Stefano,
Martin Gering, Laura Conforti

Correspondence

laura.conforti@nottingham.ac.uk

In Brief

Loreto et al. show that NAD-precursor NMN, previously reported to induce Wallerian degeneration, stimulates a Ca^{2+} rise in injured axons, which requires the protein SARM1 and shortly precedes fragmentation. Changes in mitochondrial dynamics are not associated with degeneration. These results advance our understanding of axon degeneration mechanisms relevant to neurodegeneration.

Highlights

- NMN stimulates an intra-axonal Ca^{2+} rise shortly preceding axonal fragmentation
- NMN requires SARM1 to induce Ca^{2+} rise and axon degeneration
- The extracellular environment is the main source of NMN-induced axonal Ca^{2+} rise
- Mitochondrial dynamic changes are not causative in NMN-induced degeneration



Wallerian Degeneration Is Executed by an NMN-SARM1-Dependent Late Ca²⁺ Influx but Only Modestly Influenced by Mitochondria

Andrea Loreto,¹ Michele Di Stefano,^{1,2} Martin Gering,¹ and Laura Conforti^{1,*}

¹School of Life Sciences, Medical School, University of Nottingham, NG7 2UH Nottingham, UK

²Present address: Clinical Neuroscience, UCL Institute of Neurology, Royal Free Hospital, Rowland Hill Street, NW3 2PF London, UK

*Correspondence: laura.conforti@nottingham.ac.uk

<http://dx.doi.org/10.1016/j.celrep.2015.11.032>

This is an open access article under the CC BY license (<http://creativecommons.org/licenses/by/4.0/>).

SUMMARY

Axon injury leads to rapid depletion of NAD-biosynthetic enzyme NMNAT2 and high levels of its substrate, NMN. We proposed a key role for NMN in Wallerian degeneration but downstream events and their relationship to other mediators remain unclear. Here, we show, *in vitro* and *in vivo*, that axotomy leads to a late increase in intra-axonal Ca²⁺, abolished by pharmacological or genetic reduction of NMN levels. NMN requires the pro-degenerative protein SARM1 to stimulate Ca²⁺ influx and axon degeneration. While inhibition of NMN synthesis and SARM1 deletion block Ca²⁺ rise and preserve axonal integrity, they fail to prevent early mitochondrial dynamic changes. Furthermore, depolarizing mitochondria does not alter the rate of Wallerian degeneration. These data reveal that NMN and SARM1 act in a common pathway culminating in intra-axonal Ca²⁺ increase and fragmentation and dissociate mitochondrial dysfunctions from this pathway, elucidating which steps may be most effective as targets for therapy.

INTRODUCTION

Axon degeneration is an early event contributing to symptoms in a range of age-related neurodegenerative disorders, including Parkinson's disease, Huntington's disease, Alzheimer's disease, motor neuron disease, and multiple sclerosis. Axonal damage also underpins peripheral neuropathies and is a limiting side effect of cancer chemotherapeutic agents (Conforti et al., 2014). Maintaining axon structure and function is therefore a promising therapeutic goal for these disorders.

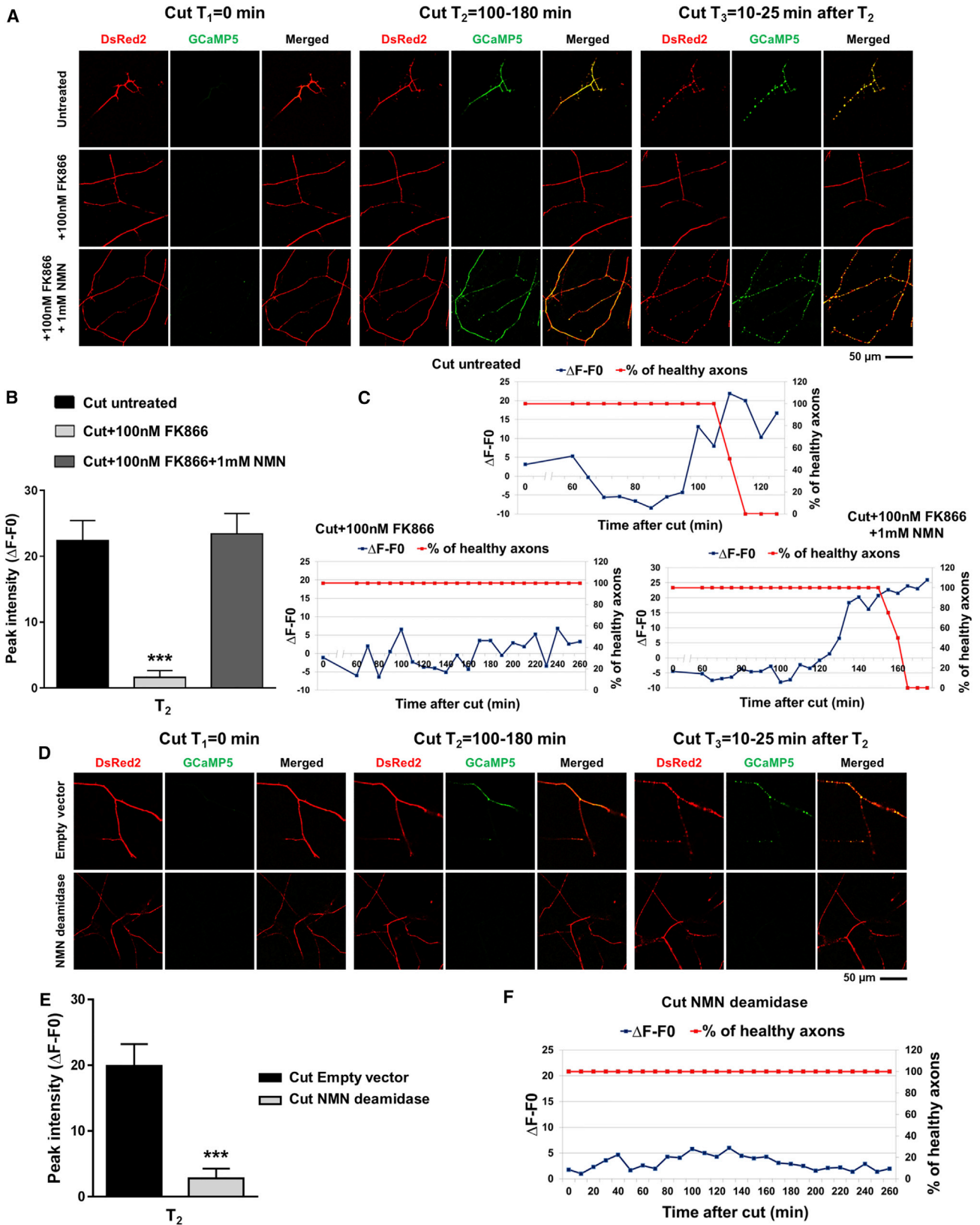
Two genetic modifications can delay by 10-fold axon degeneration after an acute injury, a process known as Wallerian degeneration (Waller, 1850), highlighting the existence of a regulated and active axon death pathway. First, expression of the neuroprotective factor Wallerian Degeneration Slow (WLD^S), a chimeric protein which fuses the nuclear isoform of the nicotinamide adenine dinucleotide (NAD)-biosynthetic enzyme nicotin-

amide mononucleotide adenylyltransferase 1 (NMNAT1) with an N-terminal sequence that relocates this enzyme from the nucleus to the cytoplasm and axons (Avery et al., 2009; Conforti et al., 2000, 2009; Mack et al., 2001). WLD^S is effective in mice, rats, *Drosophila*, zebrafish and in primary human neuronal culture (Adalbert et al., 2005; Kitay et al., 2013; Lunn et al., 1989; MacDonald et al., 2006; Martin et al., 2010), indicating strong evolutionary conservation of the axon degeneration pathway with which it interferes. WLD^S also ameliorates axon pathology and symptoms in some disease models (Conforti et al., 2014), highlighting shared mechanisms and translational potential. Remarkably, loss of the Toll-like receptor adaptor protein Sterile alpha and TIR motif containing 1 (SARM1) has the same robust protective efficacy of WLD^S. Similar to WLD^S, the protective effect of SARM1 deletion is evolutionarily conserved in mice and *Drosophila* (Osterloh et al., 2012).

It has been proposed that WLD^S delays axon degeneration by substituting for the endogenous but short-lived axonal NMNAT isoform NMNAT2, whose enzyme activity is required for axon growth and maintenance. NMNAT2 is synthesized in the cell bodies, actively transported down the axons, and rapidly degraded after injury or block of axonal transport. WLD^S, which retains the same enzymatic activity than NMNAT2 but is much more stable, prolongs axon integrity (Gilley et al., 2013; Gilley and Coleman, 2010; Milde et al., 2013).

Our previous data support a model in which WLD^S/NMNAT activity maintains axon integrity by preventing the accumulation of its substrate, the pro-degenerative NAD precursor nicotinamide mononucleotide (NMN). NMN increases after injury likely as a consequence of NMNAT2 depletion and its pharmacological or genetic inhibition strongly delays Wallerian degeneration (Di Stefano et al., 2014). The robustness of axon protection phenotype conferred by SARM1 deletion resembles that obtained by scavenging of NMN. Crucially, SARM1 depletion blocks NMNAT2 loss-induced axon degeneration but does not reduce NMN, indicating that SARM1 influences the same pathway of axon death downstream of NMN, or a convergent pathway, while other weaker modulators may join onto this pathway (Conforti et al., 2014; Gilley et al., 2015; Yang et al., 2015).

NMN increases early after injury (Di Stefano et al., 2014), leaving ample scope for downstream events, which could include an effect on intra-axonal Ca²⁺. A key role for Ca²⁺ in the late steps of degeneration, likely acting by activating



(legend on next page)

Ca²⁺-dependent proteases, has long been recognized (George et al., 1995; Wang et al., 2012). Ca²⁺ could reach the axons from the extracellular environment or originate from intra-axonal organelles (Barrientos et al., 2011; Villegas et al., 2014). Recent studies suggest instead that Ca²⁺ rise may occur early after injury (Avery et al., 2012), possibly acting upstream of SARM1 (Summers et al., 2014).

Mitochondria have been reported as central executors in Wallerian degeneration through mitochondrial permeability transition pore (mPTP) opening, which could result from a crosstalk with the endoplasmic reticulum (ER) (Barrientos et al., 2011; Villegas et al., 2014). Augmented mitochondrial motility in WLD^s could increase Ca²⁺ buffering capability and contribute to protection (Avery et al., 2012). However, Wallerian degeneration is only modestly delayed in axons devoid of mitochondria in some models and mitochondria are dispensable for WLD^s protection (Kitay et al., 2013); therefore, the role of mitochondria in Wallerian degeneration and the WLD^s mechanism as well as the relationships among NMN increase, SARM1, Ca²⁺, and mitochondrial dynamics remain unresolved.

Here we report that intra-axonal Ca²⁺ elevation after axotomy lies downstream of NMN and immediately precedes axon fragmentation. We found that SARM1 is required for NMN to initiate axon degeneration and that Ca²⁺ rise is a common downstream step. Both NMN rise inhibition and SARM1 deletion fail to prevent changes in mitochondrial dynamics occurring after axotomy, despite delaying degeneration. We also found that the rate of Wallerian degeneration is not affected by mitochondrial depolarization. By clarifying the temporal relationship between NMN rise, SARM1, Ca²⁺, and mitochondrial dynamics, our results identify critical steps of Wallerian degeneration where pharmacological intervention could be most successful.

RESULTS

Pharmacological and Genetic Data Indicate that NMN Induces a Rise in Intra-axonal Ca²⁺ Rapidly Followed by Axon Fragmentation

To address events downstream of NAD-precursor NMN (Figure S1A), which we proposed to induce axon degeneration after injury (Di Stefano et al., 2014), we first tested whether NMN accumulation evokes changes in intra-axonal Ca²⁺ concentration.

This is important since WLD^s, which blocks NMN accumulation, has been suggested to protect degenerating axons by inhibiting Ca²⁺ increase or enhancing its buffering (Adalbert et al., 2012; Avery et al., 2012). To analyze the temporal correlation between Ca²⁺ rise and axonal fragmentation, we microinjected superior cervical ganglia (SCG) neurons with plasmids encoding the Ca²⁺ indicator GCaMP5 and the fluorescent marker DsRed2. One day after microinjection, the axons were separated from the cell bodies and changes in GCaMP5 fluorescence signal in distal stumps were measured and normalized to their corresponding uncut controls (Figure 1; Figures S1B and S1C). Consistent with previous studies (Adalbert et al., 2012), we found a marked increase in Ca²⁺ levels in distal injured axons starting 2–3 hr after axotomy (Figures 1A and 1B; Movie S1). This Ca²⁺ rise just preceded the appearance of morphological damage and axon integrity was lost 10–25 min after Ca²⁺ started to increase (Figures 1A and 1C). To test whether this Ca²⁺ rise was induced by NMN accumulation, we treated axons with FK866, a potent and specific inhibitor of NMN-synthesizing enzyme NAMPT (Figure S1A). FK866 completely abolished the Ca²⁺ rise and, consistent with our previous report (Di Stefano et al., 2014), preserved axonal integrity for the entire duration of the experiment (Figures 1A–1C; Movie S1). Co-administration of NMN fully reverted the effects of FK866, restoring Ca²⁺ rise and axonal fragmentation (Figures 1A–1C; Movie S1).

We previously showed that scavenging NMN by expressing the bacterial enzyme NMN deamidase (Figure S1A; Galeazzi et al., 2011) remarkably delays axon degeneration after injury (Di Stefano et al., 2014). We then asked whether this genetic intervention to reduce NMN could also block intra-axonal Ca²⁺ rise and found that expressing NMN deamidase completely abolished this increase and preserved axonal integrity for the entire duration of the experiment (Figures 1D–1F; Movie S1).

Thus, NMN increase after injury evokes a late intra-axonal Ca²⁺ rise, which can be blocked by NAMPT inhibitor FK866 or by genetically scavenging NMN.

NMN Requires SARM1 to Induce Degeneration and Intra-axonal Ca²⁺ Increase

Because injured *Sarm1*^{-/-} nerves have high NMN levels but do not degenerate (Gilley et al., 2015), it is likely that SARM1 is required for NMN to induce axon death. We tested this possibility

Figure 1. NMN Induces a Rise in Intra-axonal Ca²⁺ Rapidly Followed by Axon Fragmentation

(A) Plasmids encoding for the Ca²⁺ indicator GCaMP5 and for the axonal marker DsRed2 were microinjected into wild-type SCG nuclei; axons were cut 1 day after microinjection and left untreated or treated as shown with FK866 and NMN, added immediately after cut. Time-lapse fluorescent images were acquired every 5 min up to 260 min. Scale bar represents 50 μm.

(B) Quantification of Ca²⁺ peak intensities (see Experimental Procedures). All measurements were normalized to uncut controls. FK866, which blocks NMN and confers protection after axotomy, completely abolished injury-induced Ca²⁺ rise; NMN addition re-established Ca²⁺ increase and reverted FK866-mediated protection. Mean ± SEM; n = 6, two fields in three independent experiments; one-way ANOVA followed by Bonferroni post hoc test; ***p < 0.001.

(C) Representative traces showing Ca²⁺ responses in axon fragments distal to the injury site over time in correlation with the percentage of healthy axons. Note that Ca²⁺ rise shortly preceded axonal fragmentation in both the untreated and FK866+NMN-treated samples. No Ca²⁺ increase was detected in the FK866-treated sample.

(D) Fluorescent images of wild-type SCG axons co-injected with plasmids encoding GCaMP5, DsRed2, and either NMN deamidase or Empty vector, at the indicated time points after transection. Scale bar represents 50 μm.

(E) Quantification of Ca²⁺ peak intensities. All measurements were normalized to uncut controls. No Ca²⁺ increase was detected in NMN deamidase expressing axons. Mean ± SEM; n = 6, two fields in three independent experiments; one-way ANOVA followed by Bonferroni post hoc test; ***p < 0.001.

(F) Representative traces showing no Ca²⁺ increase in NMN deamidase distal axon fragments in correlation with the percentage of healthy axons.

See also Figures S1 and S2.

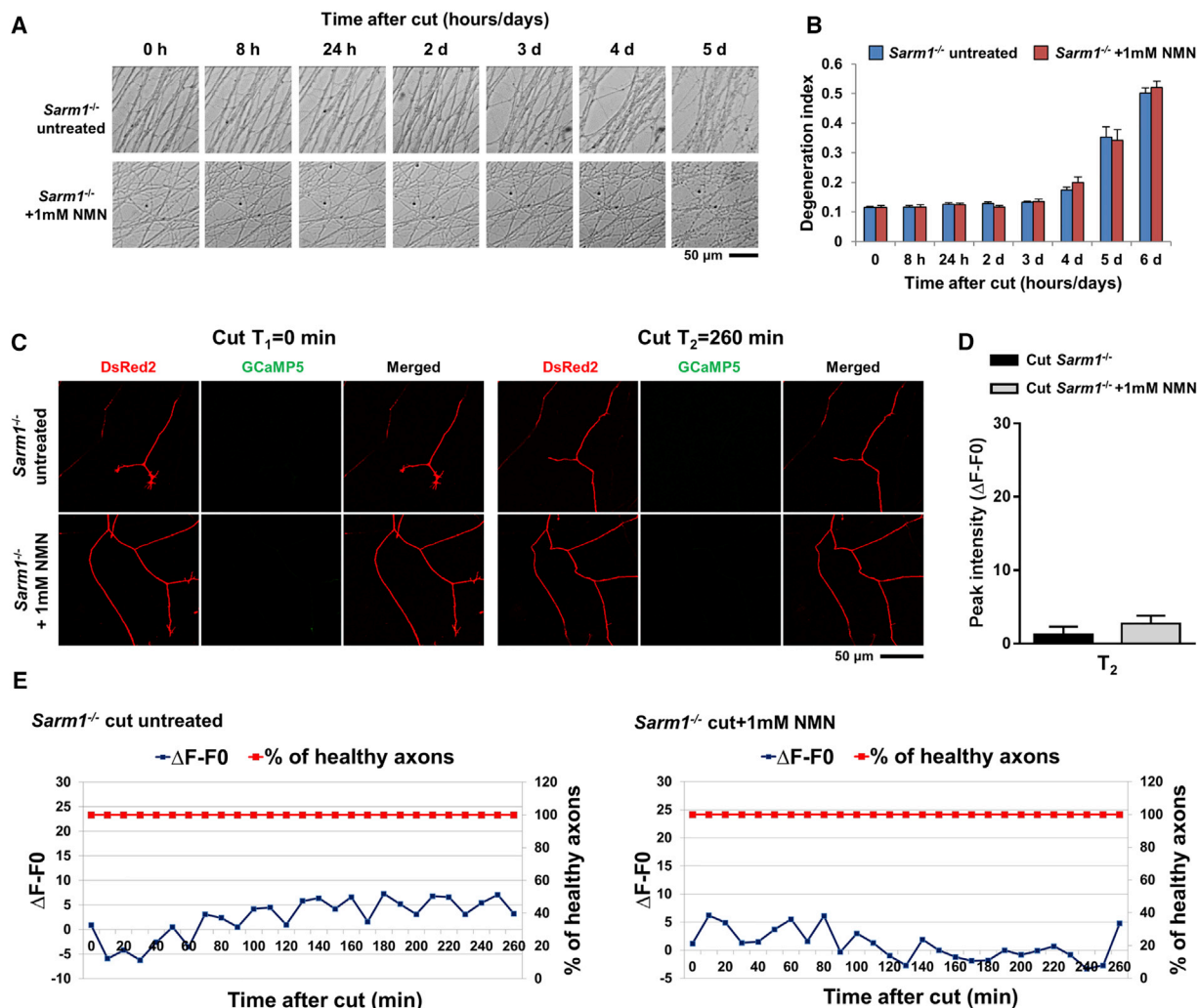


Figure 2. NMN Requires SARM1 to Induce Axon Degeneration and Ca²⁺ Rise

(A) Bright field images of *Sarm1*^{-/-} SCG axons left untreated or treated with 1 mM NMN as shown, at the indicated time points after cut. Scale bar represents 50 μ m.

(B) Degeneration index was calculated from three fields per sample in three independent experiments. Mean \pm SEM; n = 9; one-way ANOVA followed by Bonferroni post hoc test.

(C) Fluorescent images of *Sarm1*^{-/-} SCG transected axons expressing GCaMP5 and DsRed2, untreated or treated with 1 mM NMN. Scale bar represents 50 μ m.

(D) Quantification of Ca²⁺ peak intensities. All measurements were normalized to uncut controls. Mean \pm SEM; n = 6, two fields in three independent experiments; one-way ANOVA followed by Bonferroni post hoc test, p = 0.3698.

(E) Representative traces showing no increase in Ca²⁺ responses in distal *Sarm1*^{-/-} axons cut and left untreated or cut and treated with 1 mM NMN as shown, in correlation with the percentage of healthy axons.

See also Figures S1 and S2.

by adding NMN to transected *Sarm1*^{-/-} axons and found that they remained intact for at least 4 days, even in the presence of high concentrations of exogenous NMN (Figures 2A and 2B), which we even tested up to 5 mM (data not shown). In contrast, FK866-protected wild-type neurites degenerate within 3 hr when exposed to concentrations of NMN 200-fold lower (Di Stefano et al., 2014). Thus, NMN requires SARM1 to induce axon degeneration.

We then asked whether SARM1 is also required for the increase in intra-axonal Ca²⁺ after cut. This is important in view of a recent report that SARM1 acts downstream of

Ca²⁺ (Summers et al., 2014). However, in our experimental conditions we did not find any increase after axotomy in Ca²⁺ signals in the distal stumps of *Sarm1*^{-/-} axons (Figures 2C and 2D; Movie S2), which remained similar to the uninjured neurites (Figures S1D and S1E). In parallel, axonal integrity was preserved for the entire duration of the experiment (Figures 2C and 2E). NMN administration failed to induce Ca²⁺ rise in *Sarm1*^{-/-} injured axons (Figures 2C–2E; Movie S2).

Thus, SARM1 is required for NMN to induce Wallerian degeneration and Ca²⁺ increase represents a common downstream step.

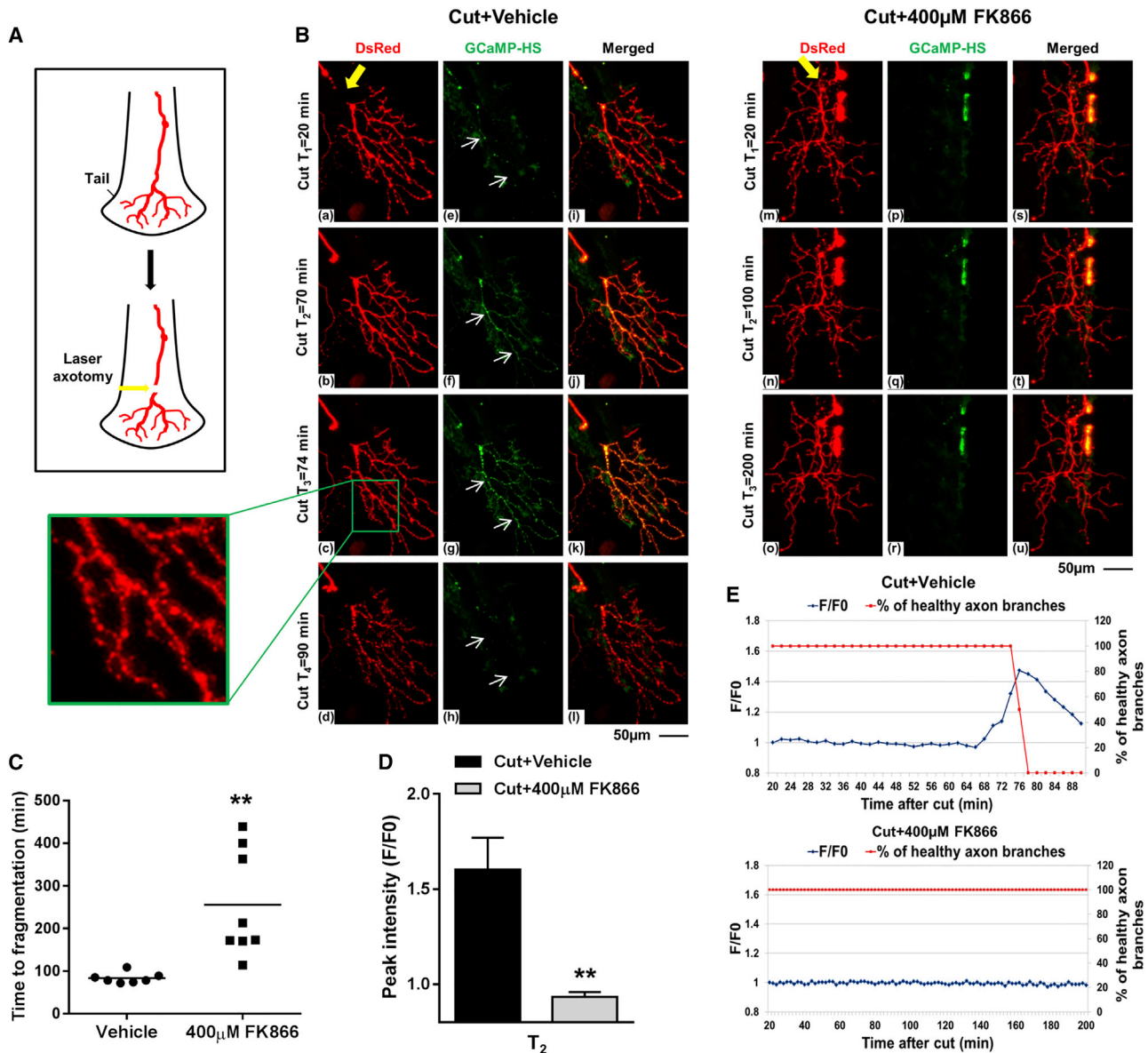


Figure 3. NMN-Synthesis Inhibitor FK866 Delays Injury-Induced Intra-axonal Ca^{2+} Increase In Vivo

(A) Schematic representation of larval zebrafish tail indicating the position of the sensory (Rohon–Beard) axons and showing the site of axotomy (yellow arrow). (B) Time-lapse fluorescent images of axons expressing DsRed and GCaMP-HS, treated with vehicle or 400 μM FK866 as shown and then transected. The yellow arrow indicates the cut site. White arrows in (f) and (g) show a clear Ca^{2+} increase immediately preceding the appearance of morphological damage. The enlargement represents the boxed area in panel (c). Scale bar represents 50 μm .

(C) Time to beginning of fragmentation following laser axotomy; each point represents one fish; horizontal bar denotes average degeneration time (Vehicle $n = 7$, FK866 $n = 8$; Student's t test; $**p < 0.01$).

(D) Quantification of Ca^{2+} peak intensities. F0 (first time point imaged) was set to 1 (mean \pm SEM; $n = 7$ –8; Student's t test; $**p < 0.01$).

(E) Representative traces showing Ca^{2+} responses distal to the injury site over time in correlation with the percentage of healthy axonal branches.

A Rapid Ca^{2+} Increase near the Injury Site Is Not Abolished in *Sarm1*^{-/-}, NMN Deamidase, or FK866-Treated Axons

An increase in intra-axonal Ca^{2+} in proximity to the cut rapidly follows the transection injury, and it is most likely due to an influx from the cut site (Adalbert et al., 2012). This immediate and localized Ca^{2+} rise leads to rapid degeneration of a short axonal

segment adjacent to the site of cut, an event known as acute axonal degeneration (Kerschensteiner et al., 2005). We recorded an early rise in Ca^{2+} levels in *Sarm1*^{-/-} axons near the cut site, followed by degeneration of short axonal segments. This was also observed in wild-type controls untreated or treated with FK866 or with FK866-NMN and in NMN deamidase-expressing axons (Figure S2) and it is consistent with direct influx of Ca^{2+}

from the injury site. This suggests that *Sarm1*^{-/-} and NMN deamidase axons, as well as axons treated with FK866, retain the capability to degenerate in response to Ca²⁺, but that this early, proximal Ca²⁺ rise is distinct from the delayed increase in the distal stump that occurs just before frank fragmentation (Figure 1).

Inhibiting NMN Synthesis with FK866 Delays Injury-Induced Intra-axonal Ca²⁺ Increase In Vivo

To assess the relationship between NMN and intra-axonal Ca²⁺ in vivo, we used zebrafish larvae 48–54 hours post-fertilization (hpf), transiently expressing DsRed along with the calcium sensor GCaMP-HS in trigeminal and Rohon–Beard somatosensory neurons. These were treated with FK866 for 6 hours prior to two-photon laser axotomy (Figures 3A and 3B). As we previously reported, FK866 strongly delays axon fragmentation in this model organism (Figures 3Bm–3Bo and 3C; Di Stefano et al., 2014). Consistent with our in vitro observations, we detected a marked Ca²⁺ increase within axons distal to the injury site (Figures 3Be–3Bh and 3D). The first signs of axon damage appeared as soon as 4 min after Ca²⁺ rise (Figures 3Ba–3Bd and 3E; Movie S3). FK866 remarkably delayed this increase in intra-axonal Ca²⁺ (Figures 3Bp, 3Br, 3D, and 3E; Movie S4) and the subsequent axon fragmentation (Figures 3Bm–3Bo, 3C, and 3E).

Thus, NMN synthesis inhibitor FK866 blocks the increase in Ca²⁺ that immediately precedes axonal fragmentation in vivo in a vertebrate model organism.

The Extracellular Environment Is the Main Source of NMN-Induced Intra-axonal Ca²⁺ Rise

Because both extracellular influx of Ca²⁺ and its release from intracellular stores have been implicated in Wallerian degeneration (Wang et al., 2012), we asked what is the primary source of the Ca²⁺ rise induced by NMN. SCG explant axons were cut and immediately treated with FK866. In order to exclude intracellular conversion of NMN to NAD mediated by any residual axonal NMNAT2, we added NMN to FK866-protected neurites 12 hr after cutting (Figure 4A), a time when little or no NMNAT2 remains (Gilley and Coleman, 2010). In these conditions, NMN induces complete degeneration of FK866-protected axons within 3 hr from its addition (Figures 4Be–4Bf and 4C; Di Stefano et al., 2014). We used EGTA to chelate extracellular Ca²⁺ and saw a remarkable delay of axon degeneration after NMN addition (Figures 4Bm–4Bp and 4C). Similar results were obtained using L-type Ca²⁺ channels blockers verapamil (Figures 4Bq–4Bt and 4C) and nifedipine (Figures S3A (i–l) and S3B). In addition, also KB-R7943, an inhibitor of the reverse Na⁺/Ca²⁺ exchanger, significantly delayed NMN-induced degeneration, although its effect was weaker (Figures 4Bu–4Bx and 4C). EGTA was protective also in dorsal root ganglion (DRG) cultures (Figure S4).

A release of Ca²⁺ from axonal ER, leading to mPTP opening and release of intra-mitochondrial Ca²⁺ has been observed in the execution phase of Wallerian degeneration (Villegas et al., 2014). Therefore, we tested whether this sequence of events is induced by NMN. We observed that ryanodine receptor antagonist ryanodine significantly delayed NMN-

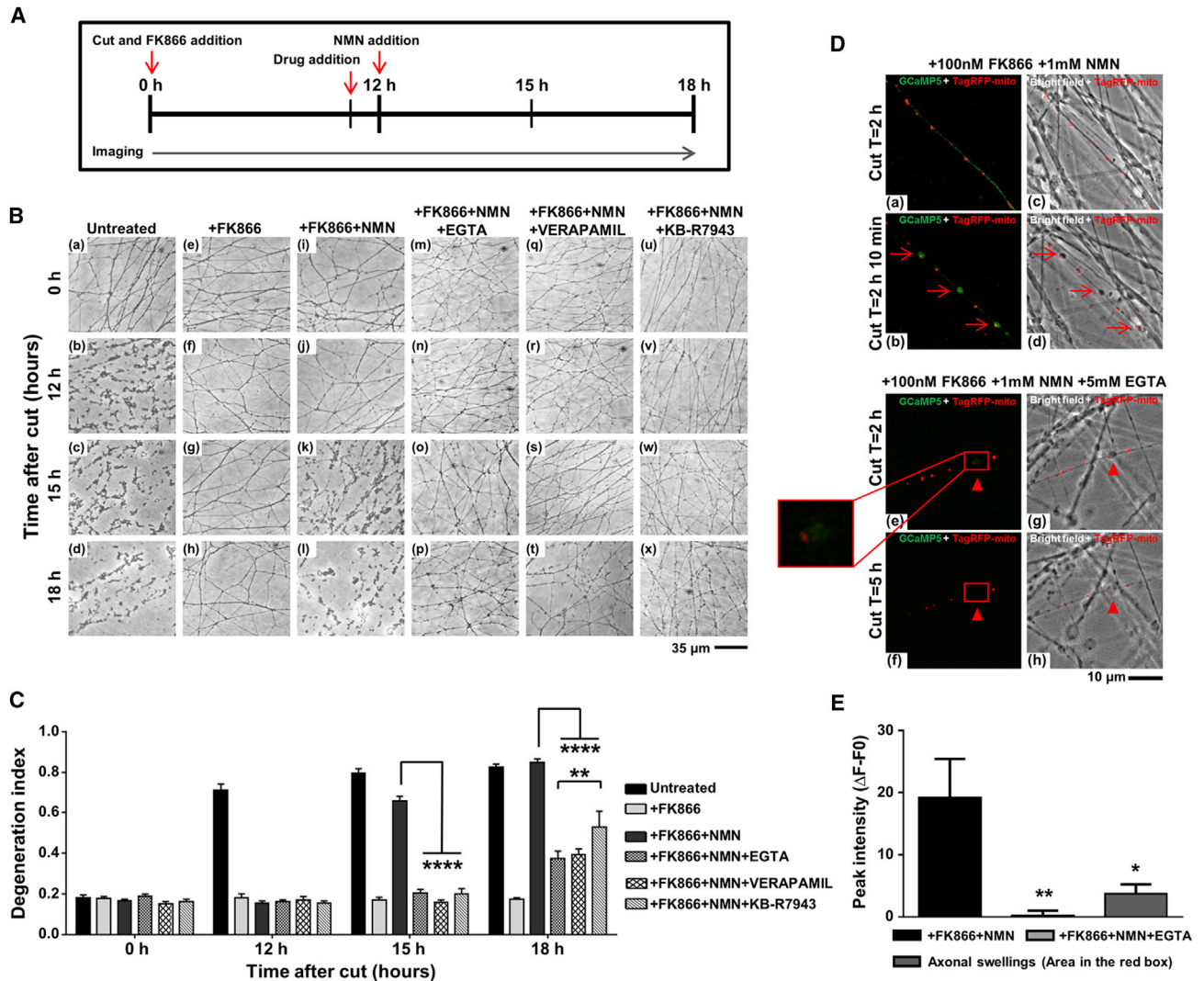
induced degeneration, although its effect was weaker than that obtained with EGTA and the other Ca²⁺-channel blockers used (Figures S3A (m–p) and S3B; Figures 4B and 4C). We also found that cyclosporine A and ruthenium red, which block mPTP opening (Barrientos et al., 2011), more modestly influence the rate of NMN-induced axon degeneration in our model (Figures S3C (i–p) and S3D). These results indicate that the main source of intra-axonal Ca²⁺ stimulated by NMN is the extracellular environment, with a weaker contribution from intracellular organelles.

To investigate the temporal relationship between Ca²⁺ influx and its internal release and to detect any Ca²⁺ increase in areas surrounding mitochondria, Ca²⁺ buffering organelles which have been proposed to release Ca²⁺ during Wallerian degeneration (Avery et al., 2012; Barrientos et al., 2011; Villegas et al., 2014), we microinjected SCG neurons with GCaMP5 and the mitochondrial marker TagRFP-mito. We then cut the axons and immediately added FK866 and NMN. As expected, NMN administration induced a diffuse intra-axonal Ca²⁺ increase in FK866-treated axons, rapidly followed by the formation of Ca²⁺-rich axonal swellings which started to appear as early as 10 min after Ca²⁺ rise (Figures 4Da, 4Db, 4Dd, and 4E; Figure S5A; see also Figure 1). Eighty percent of these swellings contained mitochondria (Figures 4Db and 4Dd). The relative Ca²⁺ fluorescence intensity inside axonal swellings was significantly higher compared to the signals measured inside adjacent axonal segments (Figures S5A and S5B), suggesting an accumulation of Ca²⁺ at the sites of morphological damage. EGTA addition drastically reduced NMN-induced Ca²⁺ rise (Figures 4De and 4E) and blocked axon degeneration (Figures 4Bm–4Bp and 4C). However, we still observed a weak increase in Ca²⁺ levels confined in some axonal areas where mitochondria were present (Figures 4De and 4E). This localized Ca²⁺ rise was considerably weaker than that observed following extracellular Ca²⁺ influx (Figure 4E); small swellings also appeared within the same confined axonal regions; nevertheless, frank degeneration of the distal axon stump was delayed for many hours (Figures 4Dg and 4Dh).

Together, these results indicate that NMN stimulates a late influx of Ca²⁺ from the extracellular environment. A more modest Ca²⁺ release from intracellular stores also occurs, but this is not sufficient to trigger fragmentation.

Changes in Mitochondrial Membrane Potential and Morphology Mark Different Stages of Axonal Degeneration

Changes in mitochondrial function and structure have been previously shown to occur after injury (Sievers et al., 2003; Villegas et al., 2014); however, it is still unclear whether mitochondria are major players, modest regulators, or simply markers of degeneration. As we previously reported early changes in mitochondrial membrane potential, an index of functionally active mitochondria, in injured neurites of young DRG cultures (Sievers et al., 2003), we asked whether these changes also occur in our SCG model of NMN-induced degeneration. Surprisingly, using the mitochondrial membrane potential indicator tetramethylrhodamine methyl ester perchlorate (TMRM), we found that



mitochondrial membrane potential remained stable for at least 4 hr after axotomy, a time point where axons still appear intact in SCG explant cultures. Similar results were observed after FK866 treatment and when NMN was re-added to FK866-treated axons ([Figures 5A](#) and [5B](#)). A visible decrease in TMRM signal only appeared 6 hr after injury, when clear signs

of degeneration were already present. FK866 abolished the drop in TMRM signal visible at this time point, which was then re-established by NMN re-addition ([Figures S5C](#) and [S5D](#)). We also found that SARM1 deletion delayed the drop in TMRM signal after injury, which remained stable up to 32 hr after axotomy ([Figures S5E](#) and [S5F](#)).

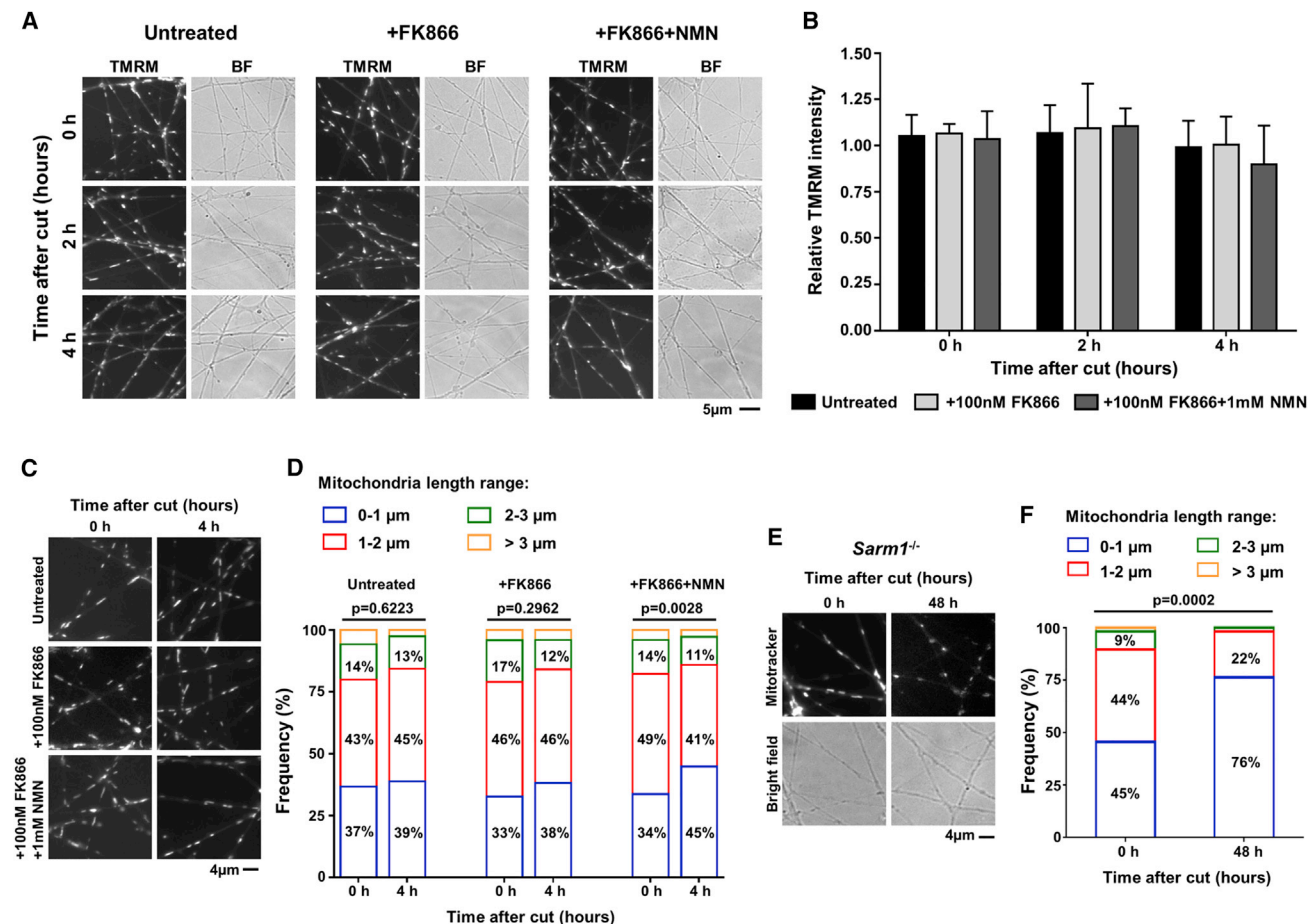


Figure 5. Changes in Mitochondrial Membrane Potential and Morphology Mark Different Stages of Axonal Degeneration

(A) Fluorescent and bright-field (BF) images of wild-type SCG axons, labeled with the mitochondrial membrane potential indicator TMRM (50 nM), at the indicated time points after cut. Where indicated, 100 nM FK866 and 1 mM NMN were added immediately after cut. Scale bar represents 5 μ m.

(B) Quantification of relative TMRM intensity (see [Experimental Procedures](#)); all measurements were normalized to uncut controls to which an arbitrary value of 1 was assigned (mean \pm SD; n = 3, one-way ANOVA followed by Bonferroni post hoc test).

(C) Fluorescent images of wild-type SCG axons, labeled with the mitochondrial marker mitotracker red, at the indicated time points after injury. Where indicated, 100 nM FK866 and 1 mM NMN were added immediately after cut. Scale bar represents 4 μ m.

(D) Quantification of mitochondrial length in wild-type SCG axons after cut. The results are expressed as the percentage of mitochondria that fall within the indicated range of length (total number of mitochondria analyzed per condition: cut untreated, 0 hr n = 359, 4 hr n = 350; Cut + FK866, 0 hr n = 410, 4 hr n = 445; cut + FK866 + NMN, 0 hr n = 362, 4 hr n = 395; Kolmogorov-Smirnov test).

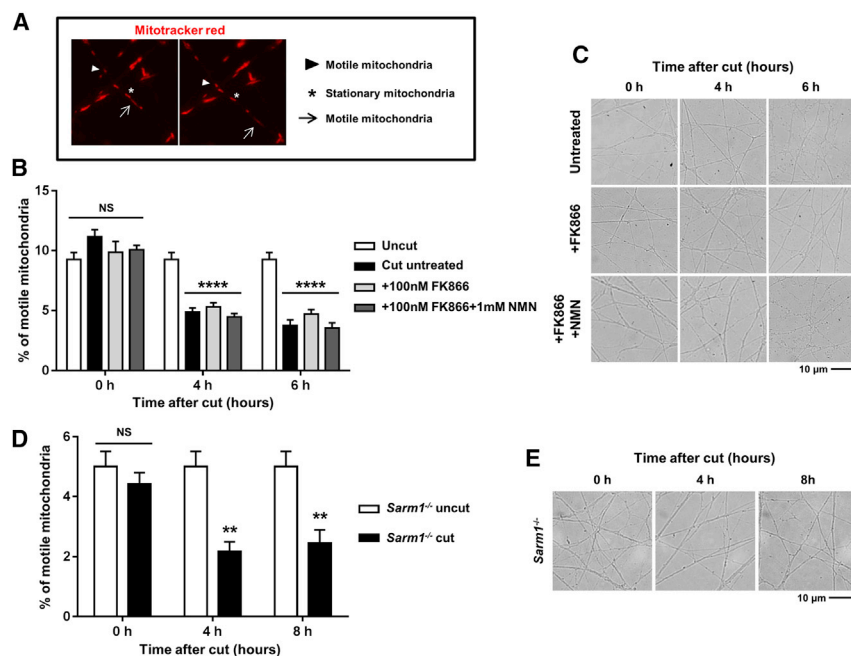
(E) Fluorescent images of *Sarm1*^{-/-} SCG axons, labeled with the mitochondrial marker mitotracker red, at the indicated time points after injury. Scale bar represents 4 μ m.

(F) Quantification of mitochondrial length in *Sarm1*^{-/-} SCG axons after cut. The results are expressed as detailed above (total number of mitochondria analyzed per condition: 0 hr n = 418, 48 hr n = 223; Kolmogorov-Smirnov test).

See also [Figure S5](#).

Mitochondrial morphological changes have been reported to be among the earliest detectable alterations during Wallerian degeneration (Vial, 1958; Webster, 1962). We thus tested whether NMN accumulation after injury could influence mitochondrial morphology. No significant change was observed among the different treatment groups in the size distribution of mitochondria immediately after cut (Figures 5C and 5D). We found a small but significant increase in the number of shorter mitochondria 4 hr after injury only in the sample treated both with FK866 and NMN. However, no change was detected in

the untreated sample, or the sample treated with FK866 alone (Figures 5C and 5D). Conversely, we observed a dramatic reduction in mitochondrial length in *Sarm1*^{-/-} axons 48 hr after injury (Figures 5E and 5F), long before frank fragmentation occurs (Figures 2A and 2B). Interestingly, we also found a significant difference (K-S p = 0.0005) in the size distribution of mitochondria between *Sarm1*^{-/-} and wild-type axons immediately after cut (compare Figures 5D and 5F), perhaps reflecting a direct influence of SARM1 on the maintenance of normal mitochondrial shape.



Thus, in this experimental system, a decrease in mitochondrial membrane potential marks the late stages of degeneration. Furthermore, while mitochondrial size is subject to modifications following an injury, these changes do not appear to correlate with the extent of degeneration.

FK866 and SARM1 Deletion Do Not Prevent Early Changes in Mitochondrial Motility after Cut

WLD^s was suggested to confer axon protection after injury by maintaining mitochondrial axonal transport, although this is a modest and short-lived effect in some studies (Avery et al., 2012; O'Donnell et al., 2013). Therefore, we next investigated whether a reduction in mitochondrial motility could underlie NMN-induced axon degeneration.

We tested whether blocking NMN synthesis with FK866 had an impact on mitochondrial dynamics after injury. To this purpose, we labeled mitochondria with the mitochondrial marker mitoracker red (Figure 6A). Consistent with previous reports (Avery et al., 2012; O'Donnell et al., 2013), we found that axotomy caused a marked reduction in the percentage of motile mitochondria 4 hr after cut in SCG explant cultures (Figure 6B; Movie S5). We also observed a decrease in the number of motile mitochondria in axons treated with FK866, similar to that in untreated cut axons (Figure 6B; Movie S5), despite FK866-treated axons maintaining their integrity during this time (Figure 6C), and for at least another 30 hr (Di Stefano et al., 2014). A similar reduction in mitochondrial motility was also observed in axons treated with both FK866 and NMN (Figure 6B; Movie S5). Interestingly, FK866-treated axons showed an almost complete arrest of mitochondrial transport 24 hr after axotomy, a time point when they still have overtly normal morphology (Movie S6).

Figure 6. FK866 and SARM1 Deletion Do Not Prevent Early Changes in Mitochondrial Motility after Cut

(A) Representative consecutive fluorescent images of SCG axons labeled with the mitochondrial marker MitoTracker Red. The arrowheads and the arrow indicate two motile mitochondria relative to a stationary mitochondria (*).

(B) Quantification of mitochondrial motility in wild-type SCG axons uncut or cut, treated as indicated and imaged at the time points shown. Percentage of motile mitochondria was calculated from two fields per sample in four different experiments (mean \pm SEM; n = 8; one-way ANOVA followed by Bonferroni post hoc test; ****p < 0.0001; NS, nonsignificant).

(C) Bright-field images of wild-type SCG axons showing axonal morphology at the indicated time points after cut. Scale bar represents 10 μ m.

(D) Quantification of mitochondrial motility in *Sarm1*^{-/-} SCG axons uncut or cut and imaged at the indicated time points. Percentage of motile mitochondria was calculated as in (B) (mean \pm SEM; n = 8; one-way ANOVA followed by Bonferroni post hoc test; **p < 0.01; NS, nonsignificant).

(E) Bright field images of *Sarm1*^{-/-} SCG axons showing axonal morphology at the indicated time points after cut. Scale bar represents 10 μ m.

We also analyzed mitochondrial transport in *Sarm1*^{-/-} SCG neurites, where protection against Wallerian degeneration is even stronger than that achieved with FK866. Remarkably, a substantial reduction in mitochondrial motility was also detected as early as 4 hr after injury, when *Sarm1*^{-/-} axons are intact (Figures 6D and 6E; Movie S7); mitochondrial transport completely stopped 48 hr after injury (Movie S8), long before axons fragment (Figures 2A and 2B).

Thus, axon protection by FK866 and SARM1 deletion is not mediated by an effect on mitochondrial dynamics.

Mitochondrial Depolarization Does Not Alter the Rate of Wallerian Degeneration

Next, we asked whether direct damage to mitochondria could affect the rate of Wallerian degeneration. This is possible because damaged mitochondria could release mediators of cell and axon death that could cause the axon demise after injury (Court and Coleman, 2012). Therefore, we treated axons with the protonophore Carbonyl cyanide m-chlorophenyl hydrazone (CCCP), which causes an uncoupling of the proton gradient and disruption of mitochondrial membrane potential (Ly et al., 2003).

When exposed to 50 μ M CCCP, mitochondria in axons immediately lost membrane potential, as shown by a remarkable, instantaneous decrease in TMRM fluorescent signal (Figure 7A). Despite this, frank axonal fragmentation only occurred 32–48 hr after CCCP addition (Figures 7A and 7B). This is a much slower time course than that of Wallerian degeneration, which in our experimental system is completed within 8 hr. This remarkable time difference enabled us to test whether mitochondrial depolarization affects the rate of Wallerian degeneration. We added CCCP to SCG explants immediately prior to axotomy (Figure 7C)

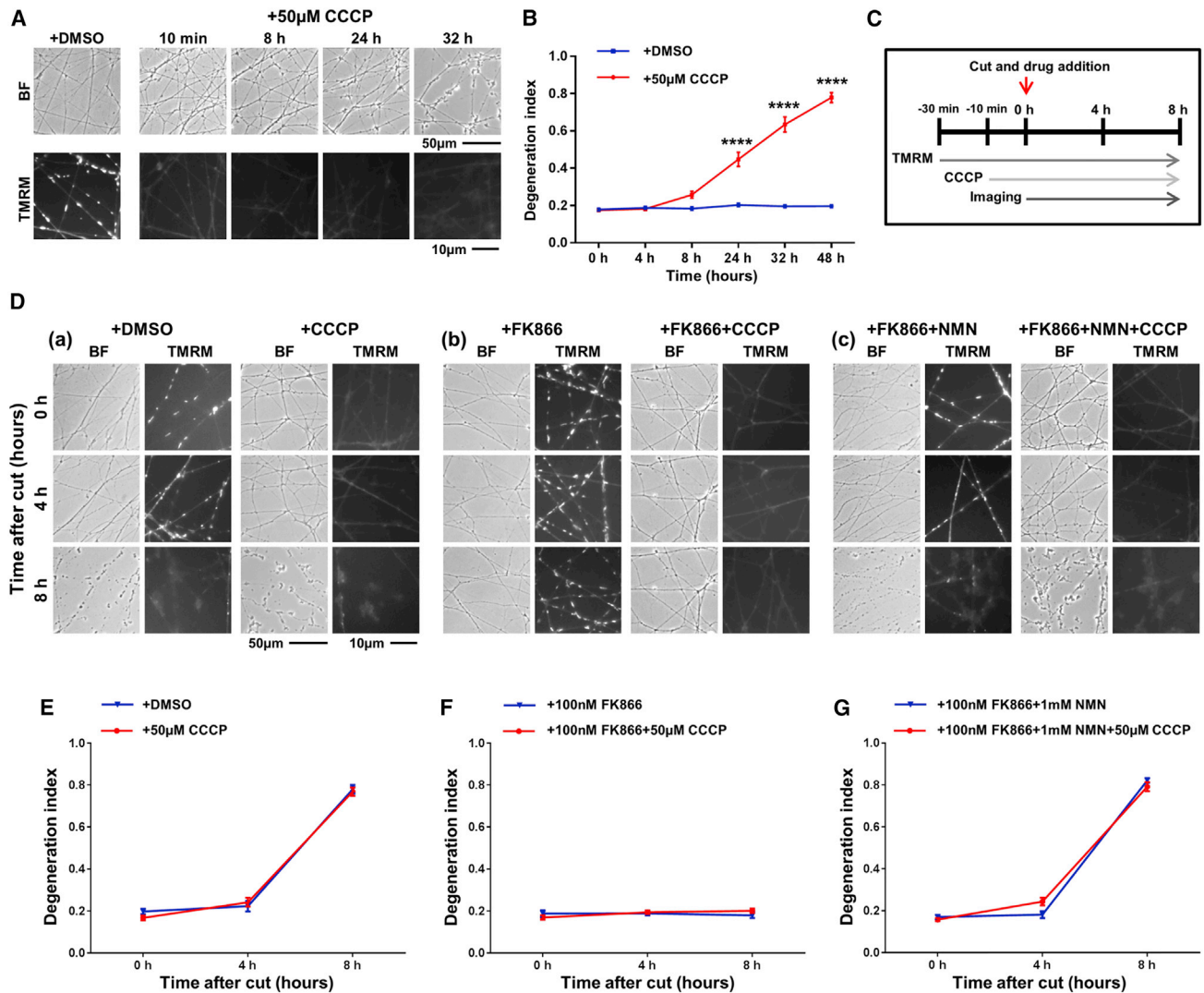


Figure 7. Mitochondrial Depolarization Does Not Alter the Rate of Wallerian Degeneration

(A) Uninjured wild-type SCG explants were treated with 50 µM CCCP or vehicle (DMSO); 50 nM TMRM was added to confirm full depolarization of axonal mitochondria following CCCP addition. Representative bright-field (BF) and representative fluorescent images of wild-type SCG axons were acquired at the indicated time points after CCCP addition. Scale bars represent 50 and 10 µm.

(B) Degeneration index was calculated from three fields per sample in six independent experiments (mean ± SEM; n = 18; one-way ANOVA followed by Bonferroni post hoc test; ****p < 0.0001).

(C) Schematic representation of the experimental design (not drawn to scale). Wild-type SCG axons were incubated with 50 nM TMRM to monitor mitochondrial membrane potential and treated with CCCP (added 10 min before axotomy) or DMSO.

(D) Representative bright-field and representative fluorescent images of transected wild-type SCG axons treated with CCCP or vehicle (DMSO) (a–c) and with 100 nM FK866 (b) or with 100 nM FK866 + 1 mM NMN (c). The dramatic loss of TMRM signal following CCCP addition confirmed full depolarization of axonal mitochondria. Scale bars represent 50 and 10 µm.

(E–G) Degeneration index was calculated from three fields per sample in three independent experiments (mean ± SEM; n = 9; one-way ANOVA followed by Bonferroni post hoc test).

See also [Figure S6](#).

and then followed the time course of axon degeneration. Despite the much earlier, almost instantaneous loss of TMRM signal, cut axons treated with CCCP underwent Wallerian degeneration at the same rate as cut, vehicle-treated axons ([Figures 7Da and 7E](#)). Furthermore, CCCP treatment did not affect axon protection conferred by FK866 or reversion by NMN administration after axotomy ([Figures 7Db, 7Dc, 7F, and](#)

[7G](#)). Similarly, the rate of axon degeneration in transected *Sarm1*^{-/-} axons treated with CCCP did not differ from that of the untreated axons, despite the rapid depolarization of *Sarm1*^{-/-} mitochondria upon CCCP addition, as expected ([Figures S6A and S6B](#)).

Together, these results dissociate the loss of mitochondrial function from the onset of Wallerian degeneration.

DISCUSSION

Our proposed model of Wallerian degeneration predicts that axonal integrity is lost as a consequence of the accumulation of the pro-degenerative molecule NMN (Di Stefano et al., 2014), whose levels in axons are normally limited by the NAD-biosynthetic enzyme NMNAT2 (Gilley and Coleman, 2010). Here, using pharmacological and genetic experimental approaches in *in vitro* mammalian primary neurons and an *in vivo* vertebrate model organism, we show that NMN initiates a Ca^{2+} -mediated execution program of axon degeneration after injury, which requires the presence of the recently identified pro-axon death protein SARM1. Furthermore, inhibition of NMN synthesis and SARM1 deletion both fail to prevent early alterations in mitochondrial motility after cut and disrupting mitochondrial membrane potential does not affect the rate of injury-induced axon degeneration; thus, a change in mitochondrial homeostasis appears to be a marker of Wallerian degeneration rather than a causative event.

Although our NMN-induced axon degeneration model is supported by pharmacological and genetic studies *in vitro* and *in vivo* (see Figures 1 and 3 and Di Stefano et al., 2014), some recent studies find instead a beneficial effect of NMN, explained by its intra-axonal conversion to NAD (Wang et al., 2015). The difference in our experimental settings (mouse intact explants instead of rat dissociated neurons) precludes a direct comparison. However, in our hands, NMN shows a rapid pro-degenerative effect when added up to 12 hr (SCG explants) or 24 hr (DRG explants) post-axotomy (see Figure 4, Figure S4, and Di Stefano et al., 2014); at these time points, NMN conversion to NAD is prevented by the complete degradation of NMNAT2, whose activity could remain in the experiments performed by (Wang et al., 2015). Careful comparison studies will need to address these discrepancies to reconcile these apparent contradictions.

Intra-axonal Ca^{2+} increase after axotomy follows a biphasic pattern, showing a first rise soon after and near the site of injury followed by second, delayed one along the whole axon length; however its temporal relationship with axonal fragmentation is still debated (Adalbert et al., 2012; Avery et al., 2012; Gerdts et al., 2011; Villegas et al., 2014; Yang et al., 2013). Our finding that NMN induces a late intra-axonal Ca^{2+} increase after injury, which is rapidly followed by axonal degeneration, are consistent with a model in which the late Ca^{2+} rise is the central and causative event marking the execution phase of degeneration on which several other mediators may converge.

Consistent with a recent report that SARM1 is required for degeneration downstream of NMNAT2 loss (Gilley et al., 2015), our data suggest that Ca^{2+} lies downstream of both NMN and SARM1 in a main, unique axon death pathway (Figure S6C; Conforti et al., 2014). A recent study proposed that SARM1 acts downstream of intra-axonal Ca^{2+} increase (Summers et al., 2014). The early Ca^{2+} rise has been suggested as a causative step in Wallerian degeneration (Avery et al., 2012). Our data, however, indicate that the early Ca^{2+} increase in the proximity of the cut site and its associated acute degeneration occur indistinguishably in wild-type rapidly degenerating axons as well in *Sarm1*^{-/-}, NMN deamidase and FK866-treated axons, all condi-

tions where Wallerian degeneration is dramatically delayed. Similarly, WLD^S does not prevent the early rise of Ca^{2+} near the cut site (Adalbert et al., 2012). Furthermore, Ca^{2+} blockers delay degeneration induced by NMN in axons injured as long as 12 hr earlier but maintained intact by FK866. Crucially, WLD^S-sensitive Wallerian degeneration can be induced without injury *in vitro* or *in vivo* by NMNAT2 selective depletion (Gilley and Coleman, 2010; Hicks et al., 2012) and does not require an influx of Ca^{2+} from the cut site to initiate it. All these observations dissociate initial Ca^{2+} influx from degeneration.

Two ways of preventing Ca^{2+} influx from the extracellular environment confer strong protection from NMN-induced axon degeneration: (1) sequestering extracellular Ca^{2+} with EGTA, and (2) blocking Ca^{2+} influx via Ca^{2+} channels. While strongly implicating extracellular Ca^{2+} in the late execution stages of Wallerian degeneration, these observations suggest that the Ca^{2+} sensitive step could be at a point where morphologically protecting axons may not restore their function. Therefore, upstream mediators of the axon death pathway may prove therapeutically more useful targets.

Extracellular Ca^{2+} influx may be due to a dysregulation of Ca^{2+} channels following a depolarization of the axonal membrane, which itself could be a consequence of energy depletion (Mishra et al., 2013; Wang et al., 2005). This could be triggered by activation of a MAPK signaling pathway by SARM1 (Yang et al., 2015) or even by a downstream effect on NAD levels (Gerdts et al., 2015). Consistent with previous reports (Barrientos et al., 2011; Villegas et al., 2014), our data also indicate a small contribution of intracellular organelles to the total intra-axonal Ca^{2+} rise after injury, noticeable following EGTA treatment (Figures 4D and 4E). Despite being insufficient to trigger fragmentation on its own in the rapid timescale of Wallerian degeneration, this could nevertheless contribute to the degeneration process. Our observation that mitochondria localize at the sites of Ca^{2+} accumulation suggests they could be one of the sources of this weaker Ca^{2+} increase. Consistently, we found a protective effect when interfering with mPTP opening (Figures S3C and S3D), even if more modest to what previously reported *ex vivo* (Barrientos et al., 2011), where Schwann cells and, more specifically, an effect of the pharmacological treatments on Schwann cell mitochondria, could have a stronger influence on axonal survival.

Whether mitochondria play a central role in Wallerian degeneration, and whether reported changes in mitochondrial shape, dynamics, and membrane potential (Avery et al., 2012; Sievers et al., 2003; Villegas et al., 2014) are a cause or consequence of degeneration or are general markers of compromised axons remain unclear. In our model of NMN-induced axon degeneration, we find that mitochondrial membrane potential drops after cut, but only when morphological damages to axons are already present, and may even be a consequence of Ca^{2+} influx. Crucially, disrupting mitochondrial membrane potential before injury does not alter the rate of degeneration or the effect of FK866 and SARM1 deletion. Consistent with our data, Wallerian degeneration occurs also in axons devoid of mitochondria and WLD^S protection is independent of axonal mitochondria (Kitay et al., 2013; Rawson et al., 2014). The depletion of other axonal proteins after injury may explain the effects on mitochondrial

homeostasis. For instance, SCG10, which is involved in the regulation of mitochondrial dynamics, is also rapidly lost after injury and its overexpression confers a modest protective phenotype (Shin et al., 2012), raising the possibility that mitochondrial changes may follow the depletion of such a regulator. In addition, mitochondrial arrest could also be a response to local Ca^{2+} changes (Wang and Schwarz, 2009). Mitochondria depend on the integrity of a nuclear-mitochondrial communication pathway regulated by NAD metabolism (Fang et al., 2014), and could be affected when this control is lost as consequence of the injury. Intriguingly, axonal mitochondria appear shorter and more static in the absence of SARM1. While supporting that Wallerian degeneration is independent of mitochondrial shape and motility, these observations raise a series of questions on the role of SARM1 in mitochondria. Indeed, SARM1 contains an N-terminal mitochondrial localization signal and is, at least in part, associated with mitochondria (Osterloh et al., 2012). SARM1 mitochondrial localization may be dispensable for the execution of Wallerian degeneration; however, it is required for viral-induced cell death (Mukherjee et al., 2013). The relevance of mitochondrial homeostasis in SARM1 biological function therefore needs to be further explored.

In our hands treatment of axons with CCCP to induce mitochondrial depolarization does not affect the rate of Wallerian degeneration, but it does initiate a slower axonal degeneration process in intact axons. A previous study showed that CCCP toxicity in uninjured axons was insensitive to WLD^s (Ikegami and Koike, 2003), which may appear in contrast to our result. However, we used CCCP at a lower concentration and, most importantly, in the context of axotomy where CCCP action could differ. Intriguingly, other reports show that mitochondrial dysfunctions activate a pathway of degeneration sensitive to regulators of Wallerian degeneration (Press and Milbrandt, 2008; Summers et al., 2014). This mechanism could be different from the axon degeneration induced by depletion of axonal mitochondria (Fang et al., 2012; Rawson et al., 2014), which in contrast is insensitive to NMNAT/WLD^s pathway (Fang et al., 2012). Furthermore, in *C. elegans* mitochondrial and transport defects leading to axon degeneration are observed as a consequence of α -tubulin acetyltransferase gene *mec-17* loss (Neumann and Hilliard, 2014). Explaining the mechanistic links between mitochondrial dysfunction-induced axon degeneration and Wallerian degeneration will be important in view of the causative role of mitochondrial dysfunction in a variety of neurodegenerative disorders characterized by axonal degeneration (Conforti et al., 2014).

In summary, our data identify crucial steps of an axon death pathway initiated by NMN accumulation. We show that NMN requires SARM1 to activate a destruction process where extracellular Ca^{2+} influx is the main executor (Figure S6C). We reveal an additional, minor contribution of mitochondrial Ca^{2+} release but our data do not support a central role for mitochondria in NMN-induced axon degeneration. Because Ca^{2+} appears to be temporally distant from the point of NMN accumulation, leaving time for signaling events, it is now important to clarify what are these signals and how NMN interacts with SARM1. These studies should help identifying effective targets to delay axon degeneration in injury and disease.

EXPERIMENTAL PROCEDURES

All studies conformed to the institution's ethical requirements in accordance with the 1986 Animals (Scientific Procedures) Act.

Explant and Dissociated Cell Cultures

C57BL/6 or CD1 (referred to as wild-type, Charles River, UK) and *Sarm1*^{-/-} (kindly provided by Dr. Michael Coleman, the Babraham Institute) mouse SCG explants, were dissected from P0-2 mouse pups and DRG explants were dissected from E16 mouse embryos. Explants were cultured for 6–7 days and then axotomized as previously described (Di Stefano et al., 2014) and as detailed in the Supplemental Experimental Procedures.

Wild-type and *Sarm1*^{-/-} SCG dissociated neurons were obtained as described (Di Stefano et al., 2014) and as detailed in Supplemental Experimental Procedures. Neurites were allowed to extend for 3 days in culture before microinjection and were axotomized the following day using a scalpel. We refer to time 0 as the first time point acquired immediately after cut.

In our experimental system (Di Stefano et al., 2014), neurites originating from wild-type SCG explants degenerate within 8 hr after cut. For the purpose of comparison, no morphological changes occur in wild-types within the first 4 hr after cut; clear morphological damages and frank fragmentation occur at 6–8 hr after cut. Neurites originating from dissociated cells degenerate within ~3 hr after cut; this difference could be due to the different time in culture (Buckmaster et al., 1995).

Microinjection

Dissociated cells were microinjected as described in (Di Stefano et al., 2014) and in the Supplemental Experimental Procedures.

Ca²⁺ Imaging and Quantification

Wild-type and *Sarm1*^{-/-} dissociated SCG neurons were cut and then imaged in a controlled environment (37°C and 5% CO₂). Treatments were applied 30 min before cut or immediately after cut and time-lapse fluorescent images and bright-field images were acquired analyzed and quantified as detailed in the Supplemental Experimental Procedures.

Ca²⁺ Imaging and Quantification in Zebrafish Larvae

Zebrafish larvae were grown, transfected, axotomized, and imaged as described (Di Stefano et al., 2014) and as detailed in the Supplemental Experimental Procedures.

SCG and DRG Explant Treatment and Acquisition of Bright-Field Images

Wild-type SCG neurites were cut and drugs were administered as described in (Di Stefano et al., 2014) and in Supplementary Methods. Bright field images were acquired and analyzed as detailed in the Supplemental Experimental Procedures.

Mitochondrial Motility Imaging and Quantification

Wild-type and *Sarm1*^{-/-} SCG explants were pre-incubated with 100nM Mitotracker red CMXRos (Invitrogen) for 15 min at 37°C before axotomy. Drug treatment and image acquisition is detailed in the Supplemental Experimental Procedures.

Quantification of mitochondrial motility was performed using the ImageJ plugin *Difference tracker* (Andrews et al., 2010). Differences in contrast between each movie were minimized by applying automated contrast normalization to all images using ImageJ.

Mitochondrial Membrane Potential and Length Quantification

For mitochondrial membrane potential, wild-type and *Sarm1*^{-/-} SCG neurons were incubated with the cell-permeant dye TMRM (VWR International) for 30 min at 37°C before axotomy and imaging. When used, 100 nM FK866 and 1mM NMN were administered immediately after axotomy. For mitochondrial length, wild-type and *Sarm1*^{-/-} SCG explants were incubated with 100 nM Mitotracker red CMXRos (Invitrogen) for 15 min at 37°C before cutting. Drug treatment, image

acquisition and image analysis are detailed in the [Supplemental Experimental Procedures](#).

CCCP Treatment

Uncut and cut wild-type or cut *Sarm1*^{-/-} SCG neurons were treated with 50 μ M CCCP or vehicle (DMSO) just prior to imaging. To check that CCCP treatment was triggering full depolarization of axonal mitochondria neurons were incubated for 30 min at 37°C with TMRM.

Statistical Analysis

Data are expressed as mean \pm SEM or SD. Statistical analysis was performed using ANOVA, Kolmogorov-Smirnov test, or Student's t test with p values less than 0.05 being considered significant for any set of data.

SUPPLEMENTAL INFORMATION

Supplemental Information includes Supplemental Experimental Procedures, six figures, and eight movies and can be found with this article online at <http://dx.doi.org/10.1016/j.celrep.2015.11.032>.

AUTHOR CONTRIBUTIONS

L.C. and A.L. conceived and designed the experiments. A.L. conducted most experiments, collected data, and conducted the analyses with the help of L.C. M.D.S. performed some of the in vitro experiments on *Sarm1*^{-/-} neurons. M.G. assisted with the zebrafish model. L.C. supervised and coordinated the research. A.L. and L.C. co-wrote the manuscript.

ACKNOWLEDGMENTS

We thank Prof. Victoria Chapman, Dr. Michael Coleman, and Dr. Jon Gilley for critically reading the manuscript and for helpful discussion; all members of the Conforti laboratory and Dr. Federico Dajas-Bailador for helpful discussion; and members of the Coleman laboratory for providing *Sarm1*^{-/-} ganglia. We thank Dr. Stefan Milde and Dr. Michael Coleman for kindly providing mitoTAG-RFP plasmid and Dr. Llewelyn Roderick for GCaMP5 construct. We thank Dr. Mauricio Vargas and Prof. Alvaro Sagasti for kindly providing UAS:GCaMP-HS and Isl1:Gal4:UAS:DsRed plasmids and for helpful discussion. We thank the members of the M.G. lab for help with the zebrafish model, and in particular Maryam Jalali. We thank Tim Self, Robert Markus, Chris Gell, and CSI/SLIM for use of imaging facilities. This study was supported by a Faculty of Medicine and Health Sciences, University of Nottingham, nonclinical senior fellowship (to L.C.); a PhD studentship of the School of Life Sciences and EURES, University of Nottingham (to A.L.); and a Marie Curie Intra European Fellowship within the 7th European Community Framework Program (to M.D.S., L.C.).

Received: March 13, 2015

Revised: September 1, 2015

Accepted: November 6, 2015

Published: December 10, 2015

REFERENCES

Adalbert, R., Gillingwater, T.H., Haley, J.E., Bridge, K., Beirowski, B., Berek, L., Wagner, D., Grumme, D., Thomson, D., Celik, A., et al. (2005). A rat model of slow Wallerian degeneration (WldS) with improved preservation of neuromuscular synapses. *Eur. J. Neurosci.* *21*, 271–277.

Adalbert, R., Morreale, G., Paizs, M., Conforti, L., Walker, S.A., Roderick, H.L., Bootman, M.D., Siklós, L., and Coleman, M.P. (2012). Intra-axonal calcium changes after axotomy in wild-type and slow Wallerian degeneration axons. *Neuroscience* *225*, 44–54.

Andrews, S., Gilley, J., and Coleman, M.P. (2010). Difference Tracker: ImageJ plugins for fully automated analysis of multiple axonal transport parameters. *J. Neurosci. Methods* *193*, 281–287.

Avery, M.A., Sheehan, A.E., Kerr, K.S., Wang, J., and Freeman, M.R. (2009). Wld S requires Nmnat1 enzymatic activity and N16-VCP interactions to suppress Wallerian degeneration. *J. Cell Biol.* *184*, 501–513.

Avery, M.A., Rooney, T.M., Pandya, J.D., Wishart, T.M., Gillingwater, T.H., Geddes, J.W., Sullivan, P.G., and Freeman, M.R. (2012). WldS prevents axon degeneration through increased mitochondrial flux and enhanced mitochondrial Ca²⁺ buffering. *Curr. Biol.* *22*, 596–600.

Barrientos, S.A., Martinez, N.W., Yoo, S., Jara, J.S., Zamorano, S., Hetz, C., Twiss, J.L., Alvarez, J., and Court, F.A. (2011). Axonal degeneration is mediated by the mitochondrial permeability transition pore. *J. Neurosci.* *31*, 966–978.

Buckmaster, E.A., Perry, V.H., and Brown, M.C. (1995). The rate of Wallerian degeneration in cultured neurons from wild type and C57BL/WldS mice depends on time in culture and may be extended in the presence of elevated K⁺ levels. *Eur. J. Neurosci.* *7*, 1596–1602.

Conforti, L., Tarlton, A., Mack, T.G., Mi, W., Buckmaster, E.A., Wagner, D., Perry, V.H., and Coleman, M.P. (2000). A Ufd2/D4Cole1e chimeric protein and overexpression of Rbp7 in the slow Wallerian degeneration (WldS) mouse. *Proc. Natl. Acad. Sci. USA* *97*, 11377–11382.

Conforti, L., Wilbrey, A., Morreale, G., Janeckova, L., Beirowski, B., Adalbert, R., Mazzola, F., Di Stefano, M., Hartley, R., Babetto, E., et al. (2009). Wld S protein requires Nmnat activity and a short N-terminal sequence to protect axons in mice. *J. Cell Biol.* *184*, 491–500.

Conforti, L., Gilley, J., and Coleman, M.P. (2014). Wallerian degeneration: an emerging axon death pathway linking injury and disease. *Nat. Rev. Neurosci.* *15*, 394–409.

Court, F.A., and Coleman, M.P. (2012). Mitochondria as a central sensor for axonal degenerative stimuli. *Trends Neurosci.* *35*, 364–372.

Di Stefano, M., Nascimento-Ferreira, I., Orsomando, G., Mori, V., Gilley, J., Brown, R., Janeckova, L., Vargas, M.E., Worrell, L.A., Loreto, A., et al. (2014). A rise in NAD precursor nicotinamide mononucleotide (NMN) after injury promotes axon degeneration. *Cell Death Differ.*

Fang, Y., Soares, L., Teng, X., Geary, M., and Bonini, N.M. (2012). A novel Drosophila model of nerve injury reveals an essential role of Nmnat in maintaining axonal integrity. *Curr. Biol.* *22*, 590–595.

Fang, E.F., Scheibye-Knudsen, M., Brace, L.E., Kassahun, H., SenGupta, T., Nilsen, H., Mitchell, J.R., Croteau, D.L., and Bohr, V.A. (2014). Defective mitophagy in XPA via PARP-1 hyperactivation and NAD(+)/SIRT1 reduction. *Cell* *157*, 882–896.

Galeazzi, L., Bocci, P., Amici, A., Brunetti, L., Ruggieri, S., Romine, M., Reed, S., Osterman, A.L., Rodionov, D.A., Sorci, L., and Raffaelli, N. (2011). Identification of nicotinamide mononucleotide deamidase of the bacterial pyridine nucleotide cycle reveals a novel broadly conserved amidohydrolase family. *J. Biol. Chem.* *286*, 40365–40375.

George, E.B., Glass, J.D., and Griffin, J.W. (1995). Axotomy-induced axonal degeneration is mediated by calcium influx through ion-specific channels. *J. Neurosci.* *15*, 6445–6452.

Gerdts, J., Sasaki, Y., Vohra, B., Marasa, J., and Milbrandt, J. (2011). Image-based screening identifies novel roles for IkkappaB kinase and glycogen synthase kinase 3 in axonal degeneration. *J. Biol. Chem.* *286*, 28011–28018.

Gerdts, J., Brace, E.J., Sasaki, Y., DiAntonio, A., and Milbrandt, J. (2015). SARM1 activation triggers axon degeneration locally via NAD⁺ destruction. *Science* *348*, 453–457.

Gilley, J., and Coleman, M.P. (2010). Endogenous Nmnat2 is an essential survival factor for maintenance of healthy axons. *PLoS Biol.* *8*, e1000300.

Gilley, J., Adalbert, R., Yu, G., and Coleman, M.P. (2013). Rescue of peripheral and CNS axon defects in mice lacking NMNAT2. *J. Neurosci.* *33*, 13410–13424.

Gilley, J., Orsomando, G., Nascimento-Ferreira, I., and Coleman, M.P. (2015). Absence of SARM1 rescues development and survival of NMNAT2-deficient axons. *Cell Rep.* *10*, 1974–1981.

Hicks, A.N., Lorenzetti, D., Gilley, J., Lu, B., Andersson, K.E., Miligan, C., Overbeek, P.A., Oppenheim, R., and Bishop, C.E. (2012). Nicotinamide

- mononucleotide adenyltransferase 2 (Nmnat2) regulates axon integrity in the mouse embryo. *PLoS ONE* 7, e47869.
- Ikegami, K., and Koike, T. (2003). Non-apoptotic neurite degeneration in apoptotic neuronal death: pivotal role of mitochondrial function in neurites. *Neuroscience* 122, 617–626.
- Kerschensteiner, M., Schwab, M.E., Lichtman, J.W., and Misgeld, T. (2005). In vivo imaging of axonal degeneration and regeneration in the injured spinal cord. *Nat. Med.* 11, 572–577.
- Kitay, B.M., McCormack, R., Wang, Y., Tsoulfas, P., and Zhai, R.G. (2013). Mislocalization of neuronal mitochondria reveals regulation of Wallerian degeneration and NMNAT/WLD(S)-mediated axon protection independent of axonal mitochondria. *Hum. Mol. Genet.* 22, 1601–1614.
- Lunn, E.R., Perry, V.H., Brown, M.C., Rosen, H., and Gordon, S. (1989). Absence of Wallerian Degeneration does not Hinder Regeneration in Peripheral Nerve. *Eur. J. Neurosci.* 1, 27–33.
- Ly, J.D., Grubb, D.R., and Lawen, A. (2003). The mitochondrial membrane potential ($\Delta\psi$) in apoptosis; an update. *Apoptosis* 8, 115–128.
- MacDonald, J.M., Beach, M.G., Porpiglia, E., Sheehan, A.E., Watts, R.J., and Freeman, M.R. (2006). The *Drosophila* cell corpse engulfment receptor Draper mediates glial clearance of severed axons. *Neuron* 50, 869–881.
- Mack, T.G., Reiner, M., Beirowski, B., Mi, W., Emanuelli, M., Wagner, D., Thomson, D., Gillingwater, T., Court, F., Conforti, L., et al. (2001). Wallerian degeneration of injured axons and synapses is delayed by a *Ube4b/Nmnat* chimeric gene. *Nat. Neurosci.* 4, 1199–1206.
- Martin, S.M., O'Brien, G.S., Portera-Cailliau, C., and Sagasti, A. (2010). Wallerian degeneration of zebrafish trigeminal axons in the skin is required for regeneration and developmental pruning. *Development* 137, 3985–3994.
- Milde, S., Gilley, J., and Coleman, M.P. (2013). Subcellular localization determines the stability and axon protective capacity of axon survival factor Nmnat2. *PLoS Biol.* 11, e1001539.
- Mishra, B., Carson, R., Hume, R.I., and Collins, C.A. (2013). Sodium and potassium currents influence Wallerian degeneration of injured *Drosophila* axons. *J. Neurosci.* 33, 18728–18739.
- Mukherjee, P., Woods, T.A., Moore, R.A., and Peterson, K.E. (2013). Activation of the innate signaling molecule MAVS by bunyavirus infection upregulates the adaptor protein SARM1, leading to neuronal death. *Immunity* 38, 705–716.
- Neumann, B., and Hilliard, M.A. (2014). Loss of MEC-17 leads to microtubule instability and axonal degeneration. *Cell Rep.* 6, 93–103.
- O'Donnell, K.C., Vargas, M.E., and Sagasti, A. (2013). WldS and PGC-1 α regulate mitochondrial transport and oxidation state after axonal injury. *J. Neurosci.* 33, 14778–14790.
- Osterloh, J.M., Yang, J., Rooney, T.M., Fox, A.N., Adalbert, R., Powell, E.H., Sheehan, A.E., Avery, M.A., Hackett, R., Logan, M.A., et al. (2012). dSarm/Sarm1 is required for activation of an injury-induced axon death pathway. *Science* 337, 481–484.
- Press, C., and Milbrandt, J. (2008). Nmnat delays axonal degeneration caused by mitochondrial and oxidative stress. *J. Neurosci.* 28, 4861–4871.
- Rawson, R.L., Yam, L., Weimer, R.M., Bend, E.G., Hartwig, E., Horvitz, H.R., Clark, S.G., and Jorgensen, E.M. (2014). Axons degenerate in the absence of mitochondria in *C. elegans*. *Curr. Biol.* 24, 760–765.
- Shin, J.E., Miller, B.R., Babetto, E., Cho, Y., Sasaki, Y., Qayum, S., Russler, E.V., Cavalli, V., Milbrandt, J., and DiAntonio, A. (2012). SCG10 is a JNK target in the axonal degeneration pathway. *Proc. Natl. Acad. Sci. USA* 109, E3696–E3705.
- Sievers, C., Platt, N., Perry, V.H., Coleman, M.P., and Conforti, L. (2003). Neurites undergoing Wallerian degeneration show an apoptotic-like process with Annexin V positive staining and loss of mitochondrial membrane potential. *Neurosci. Res.* 46, 161–169.
- Summers, D.W., DiAntonio, A., and Milbrandt, J. (2014). Mitochondrial dysfunction induces Sarm1-dependent cell death in sensory neurons. *J. Neurosci.* 34, 9338–9350.
- Vial, J.D. (1958). The early changes in the axoplasm during wallerian degeneration. *J. Biophys. Biochem. Cytol.* 4, 551–555.
- Villegas, R., Martinez, N.W., Lillo, J., Pihan, P., Hernandez, D., Twiss, J.L., and Court, F.A. (2014). Calcium release from intra-axonal endoplasmic reticulum leads to axon degeneration through mitochondrial dysfunction. *J. Neurosci.* 34, 7179–7189.
- Waller, A. (1850). Experiments on the section of glossopharyngeal and hypoglossal nerves of the frog and observations of the alternatives produced thereby in the structure of their primitive fibres. *Philos. Trans. R. Soc. Lond. B Biol. Sci.* 140, 423–429.
- Wang, X., and Schwarz, T.L. (2009). The mechanism of Ca²⁺-dependent regulation of kinesin-mediated mitochondrial motility. *Cell* 136, 163–174.
- Wang, J., Zhai, Q., Chen, Y., Lin, E., Gu, W., McBurney, M.W., and He, Z. (2005). A local mechanism mediates NAD-dependent protection of axon degeneration. *J. Cell Biol.* 170, 349–355.
- Wang, J.T., Medress, Z.A., and Barres, B.A. (2012). Axon degeneration: molecular mechanisms of a self-destruction pathway. *J. Cell Biol.* 196, 7–18.
- Wang, J.T., Medress, Z.A., Vargas, M.E., and Barres, B.A. (2015). Local axonal protection by WldS as revealed by conditional regulation of protein stability. *Proc. Natl. Acad. Sci. USA* 112, 10093–10100.
- Webster, H.D. (1962). Transient, focal accumulation of axonal mitochondria during the early stages of wallerian degeneration. *J. Cell Biol.* 12, 361–383.
- Yang, J., Weimer, R.M., Kallop, D., Olsen, O., Wu, Z., Renier, N., Uryu, K., and Tessier-Lavigne, M. (2013). Regulation of axon degeneration after injury and in development by the endogenous calpain inhibitor calpastatin. *Neuron* 80, 1175–1189.
- Yang, J., Wu, Z., Renier, N., Simon, D.J., Uryu, K., Park, D.S., Greer, P.A., Tournier, C., Davis, R.J., and Tessier-Lavigne, M. (2015). Pathological axonal death through a MAPK cascade that triggers a local energy deficit. *Cell* 160, 161–176.